Vol 15 No 3, March 2006
1009-1963/2006/15(03)/0513-05

Chinese Physics

© 2006 Chin. Phys. Soc.
and IOP Publishing Ltd

Relation between the complex Ginzburg–Landau equation and reaction–diffusion system*

Shao Xin(邵 昕), Ren Yi(任 毅), and Ouyang Qi(欧阳颀)†

Department of Physics, Peking University, Beijing 100871, *China*

(Received 14 September 2005; revised manuscript received 14 September 2005)

The complex Ginzburg–Landau equation (CGLE) has been used to describe the travelling wave behaviour in reaction–diffusion (RD) systems. We argue that this description is valid only when the RD system is close to the Hopf bifurcation, and is not valid when a RD system is away from the onset. To test this, we study spirals and anti-spirals in the chlorite-iodide-malonic acid (CIMA) reaction and the corresponding CGLE. Numerical simulations confirm that the CGLE can only be applied to the CIMA reaction when it is very near the Hopf onset.

Keywords: complex Ginzburg–Landau equation, reaction–diffusion system, chlorite-iodide-malonic acid

PACC: 0547, 0565

1. Introduction

The complex Ginzburg–Landau equation (CGLE)[1] is one of the most-studied nonlinear dynamic equations in the physics community. In pattern formation theory, it describes the dynamics of generic spatially extended systems which undergoes a supercritical Hopf bifurcation from a stationary state to an oscillatory state.[2] With the classic reductive perturbation method, any reaction-diffusion system that is close to this bifurcation can be deduced to the CGLE, which has the following form:[3,4]

$$\frac{\partial W}{\partial t} = W - (1 + \mathrm{i}\alpha)W \mid W \mid^2 + (1 + \mathrm{i}\beta)\nabla^2 W, \quad (1)$$

where W represents the complex amplitude of the oscillations; i is the imaginary unit and $\nabla^2 = (\partial^2/\partial x^2 + \partial^2/\partial y^2)$ denotes the two-dimensional Laplace operator.

In one of recent papers, the CGLE is used to explore spiral behaviour in the Fitz-Hugh–Nagumo (FHN) model.[5] Inwardly rotating waves, termed anti-spirals, have been reported.[6,7] The authors pointed out a continuous transition from spirals to anti-spirals at the wave number $k = 0$. In the succeeding papers on anti-spiral formation,[8−10] it was indicated that anti-spirals will occur when the group velocity (v_{gr}) and the phase velocity (v_{ph}) have opposite signs. Furthermore, the other transition line with the frequency $\omega = 0$ from spirals to anti-spirals has been found in the CGLE.

While the mechanism of anti-spirals in the CGLE has been well documented, more and more works show that the pattern behaviour in reaction–diffusion (RD) system exhibits qualitative difference from the corresponding CGLE. In order to clarify this observation, we explore the transition between spirals and anti-spirals in both the chlorite-iodide-malonic acid (CIMA) reaction and the CGLE.[11] In this paper, we first analytically derive the CGLE coefficients from the CIMA reaction kinetics, then conduct numerical simulations in both the CIMA RD system and the CGLE system. The behaviour of the systems, especially the onset of the transition from spirals to anti-spirals is compared, this information helps us to justify the region of usefulness of the CGLE in RD systems.

2. Model analysis

The CIMA reaction mechanism in an homogeneous RD medium can be quantitatively described by

*Project supported by the National Natural Science Foundation of China (Grant No 10274003) and the Department of Science and Technology of China.

†To whom correspondence should be addressed. E-mail: qi@pku.edu.cn

a two-variable activator-inhibitor model:[12−14]

$$\begin{aligned}\partial x/\partial t =& k_1' - k_2' x - \frac{4k_3' xy}{(u+x^2)} + D_x \nabla_r^2 x,\\ \partial y/\partial t =& k_2' x - \frac{k_3' xy}{(u+x^2)} + D_y \nabla_r^2 y,\end{aligned} \tag{2}$$

where $x = \mathrm{I}^-$ stands for the concentration of iodide, the activator; $y = \mathrm{ClO}_2^-$ represents the concentration of chlorite, the inhibitor; k_1', k_2', k_3' are reaction rate constants; u denotes a phenomenological parameter; D_x and D_y are the diffusion coefficients of I^- and ClO_2^-, respectively.

The above equations can be transformed to the following dimensionless equations:

$$\begin{aligned}\partial x'/\partial \tau &= a - x' - 4x'y'/(1+x'^2) + D_{x'} \nabla_{r'}^2 x',\\ \partial y'/\partial \tau &= b[x' - x'y'/(1+x'^2)] + D_{y'} \nabla_{r'}^2 y',\end{aligned} \tag{3}$$

where

$$\begin{aligned} &x = \mu x' \quad && y = \nu y' && t = \gamma \tau,\\ &r = 10^{-2}\, r' && a = k_1' \gamma/\mu && b = \mu/\nu,\\ &\mu = u^{\frac{1}{2}} && \gamma = 1/k_2' && \nu = u k_2'/k_3'. \end{aligned} \tag{4}$$

There exists an unique uniform steady state (x_0', y_0') solution of Eqs.(3) given by

$$(x_0', y_0') = (a/5, 1 + a^2/25). \tag{5}$$

If one chooses b as the control parameter and keeping a constant, the linear stability analysis of the fixed point (x_0', y_0') shows that the steady state becomes unstable and undergoes a transition to a state of periodic oscillations if $b < b_\mathrm{c}$, where

$$b_\mathrm{c} = 3a/5 - 25/a. \tag{6}$$

This transition is called the Hopf bifurcation, which induces periodic oscillations of the concentrations in the RD system, with an oscillation amplitude $|A|$ and an intrinsic frequency $\omega_\mathrm{c} = \sqrt{\dfrac{5(3x_0'^2 - 5)}{1 + x_0'^2}}$ $(a > 5\sqrt{5/3})$ at onset.

Using the reductive perturbation method[3,4] and after an intensive analytical study, we derived an equation for the amplitude A of the RD system. It has the following form:

$$\begin{aligned}\frac{\partial A}{\partial \tau} =& (a_1 + \mathrm{i}a_2)(b - b_\mathrm{c})A + (\alpha_1 + \mathrm{i}\alpha_2)|A|^2 A\\ &+ (\beta_1 + \mathrm{i}\beta_2)\nabla_{r'}^2 A,\end{aligned} \tag{7}$$

where

$$\begin{aligned} a_1 =& \frac{-x_0'}{2(1+x_0'^2)},\\ a_2 =& \frac{x_0'}{2(3x_0'^2 - 5)},\\ \beta_1 =& \frac{D_{x'} + D_{y'}}{2},\\ \beta_2 =& \frac{D_{x'} - D_{y'}}{10}\ \omega_\mathrm{c},\\ \alpha_1 =& \frac{2x_0'^4 - 27x_0'^2 - 5}{2x_0'^2(1+x_0'^2)^2}\\ \alpha_2 =& \frac{26x_0'^6 - 119x_0'^4 + 100x_0'^2 - 75}{30x_0'^2(3x_0'^2 - 5)(1+x_0'^2)^2}\ \omega_\mathrm{c}. \end{aligned} \tag{8}$$

Note that Eq.(7) has a saturated nonzero steady state solution only when $\alpha_1 < 0$ or $2x_0'^4 - 27x_0'^2 - 5 < 0$, which is the condition for the supercritical Hopf bifurcation. If $\alpha_1 > 0$, no saturated steady state solution can be found for Eq.(7). One has to include higher order terms to get an correct amplitude equation, which is a case of the subcritical Hopf bifurcation. In the latter case the CGLE of Eq.(1) can not be applied. Thus, the necessary conditions for Eq.(7) to describe the dynamic behaviour of the CIMA RD system are $a > 5\sqrt{5/3}$ (Hopf bifurcation) and $a < 18.495$ (supercritical).

Assuming $5\sqrt{5/3} < a < 18.495$, we can re-scale the Eq.(7) as the following:

$$\begin{aligned} A =& \sqrt{\frac{-a_1(b - b_\mathrm{c})}{\alpha_1}} \exp\left(\mathrm{i}\frac{a_2}{a_1} t\right) W,\\ r' =& \sqrt{\frac{\beta_1}{a_1(b - b_\mathrm{c})}}\ r,\\ \tau =& \frac{1}{a_1(b - b_\mathrm{c})}\ t, \end{aligned} \tag{9}$$

which gives the CGLE of Eq.(1) with coefficients

$$\begin{aligned} \alpha =& \frac{26x_0'^6 - 119x_0'^4 + 100x_0'^2 - 75}{15(3x_0'^2 - 5)(2x_0'^4 - 27x_0'^2 - 5)}\ \omega_\mathrm{c},\\ \beta =& \frac{D_{x'} - D_{y'}}{5(D_{x'} + D_{y'})}\ \omega_\mathrm{c}. \end{aligned} \tag{10}$$

In summary, using perturbation analysis and assuming the CIMA RD system is near the supercritical Hopf bifurcation, we link this RD system to the CGLE. More importantly, the control parameters in the CIMA reaction are directly mapped to the control parameters α and β in the CGLE, allowing us to compare the two systems quantitatively.

Certain background information needs to be presented before the comparison. Solutions (x', y') in

Eqs.(3) near the supercritical Hopf bifurcation with frequency ω_c can be decomposed as[3,4]

$$\begin{pmatrix} x' \\ y' \end{pmatrix} = \begin{pmatrix} x'_0 \\ y'_0 \end{pmatrix} + \begin{pmatrix} x'_1 \\ y'_1 \end{pmatrix} A(\boldsymbol{r}', \tau) e^{i\omega_c \tau} + \text{c.c.}, \tag{11}$$

where $\begin{pmatrix} x'_0 \\ y'_0 \end{pmatrix}$ is the stationary solution that loses stability at the bifurcation onset; $\begin{pmatrix} x'_1 \\ y'_1 \end{pmatrix}$ is the eigenmode of the Hopf bifurcation. The evolution of the complex amplitude $A(\boldsymbol{r}', \tau) = \sqrt{-\frac{a_1(b-b_c)}{\alpha_1}} W(\boldsymbol{r}, t) e^{ic_0 t}$ of the oscillations is described by the CGLE of Eq.(1), which has a travelling wave solution of the form

$$W(\boldsymbol{r}, t) = F(r) e^{i(k_{CGLE} r - \omega_{CGLE} t)}. \tag{12}$$

The selected wave number k_{CGLE} is a function of parameters α and β given by the nonlinear eigenvalue. It has been proved that k_{CGLE} takes the same sign as $\beta - \alpha$. The corresponding frequency ω_{CGLE} is $\omega_{CGLE} = \alpha + (\beta - \alpha) k_{CGLE}^2$.

If we translate the above analytical results to the CIMA RD system, we can deduce that there exists a travelling wave solution in this system; the wave number of the travelling waves should be:

$$k_{CIMA} = \sqrt{\frac{a_1(b-b_c)}{\beta_1}}\, k_{CGLE}, \tag{13}$$

and the frequency ω_{CIMA} should be

$$\omega_{CIMA} = (\omega_{CGLE} - a_2/a_1) a_1 (b - b_c) - \omega_c. \tag{14}$$

Propagation of small perturbations of the waves is described by the group velocity

$$\begin{aligned} v_{gr} =& \partial \omega_{CIMA} / \partial k_{CIMA} \\ =& 2\sqrt{\frac{a_1(b-b_c)}{\beta_1}}\, (\beta - \alpha)\, k_{CGLE}. \end{aligned} \tag{15}$$

Note that since the wavenumber k_{CGLE} takes the same sign as $\beta - \alpha$,[15] the group velocity is positive, which means that any small perturbation of the (anti) spiral should be pushed away from the core region.

However, the phase and group velocities do not necessarily point to the same direction. The phase waves move outward (inward) for positive (negative) phase velocity:

$$\begin{aligned} v_{ph} =& \omega_{CIMA} / k_{CIMA} \\ =& [(\omega_{CGLE} - a_2/a_1) a_1 (b - b_c) - \omega_c] / k_{CIMA} \\ \approx& -\omega_c \sqrt{\frac{\beta_1}{a_1(b-b_c)}} / k_{CGLE}. \end{aligned} \tag{16}$$

The above equation shows that v_{ph} changes sign only when k_{CGLE} changes sign, i.e., when $\alpha = \beta$. In other words, anti-spirals should be observed when $\beta > \alpha$ in the CIMA RD system. This result is consistent with the analysis of the CGLE. On the other hand, $\omega = 0$ predicted by the CGLE is no longer the spiral to anti-spiral transition line in the CIMA.

3. Simulation results

We should emphasize that the theoretical result presented in Section 2 is based on perturbation analysis. It is valid only when the system is close to the supercritical Hopf bifurcation. If the reaction goes far enough away from the onset of the instability, it should not be described by the above theory. In this case, the CGLE and the real CIMA reaction will have qualitative difference, so that the CGLE should not be used to explore the dynamics of the CIMA reaction any more. In this section, we use the spiral–anti-spiral transition as the qualitative criterion to identify this difference.

We first selected some points close to the supercritical Hopf bifurcation curve in the CIMA RD system ($b = 0.8$, $b_c = 1.17$) to compare its behaviour with the corresponding CGLE. In this case, our simulation results show that the analysis presented in the last section is valid. The behaviour of the stable travelling waves splits into two regimes, spirals for $\beta < \alpha$ and anti-spirals for $\beta > \alpha$. Figure 1 gives one example for each case. When $a = 7.5$, $b = 0.8$, $D_{x'} = 0.07$ and $D_{y'} = 0.095$, Eq.(10) gives $\alpha = 0.176$ and $\beta = -0.05$. These two parameters are within the spiral regime because $\beta < \alpha$. Consistent with this prediction, a direct numerical simulation of the dimensionless CIMA model shows the spiral in Fig.1(a). Figure 1(c) shows the corresponding time–space behaviour of the spiral. In the other case, when we select $a = 16.0$, $b = 8.0$, $D_{x'} = 0.07$ and $D_{y'} = 0.075$ in CIMA RD system, Eq.(10) gives $\alpha = -2.002$ and $\beta = 0.117$. These two parameters are within the anti-spiral regime because $\beta > \alpha$. A direct numerical simulation of the dimensionless CIMA model shows the anti-spirals in Fig.1(b) and Fig.1(d), which also agree with the theoretical

prediction.

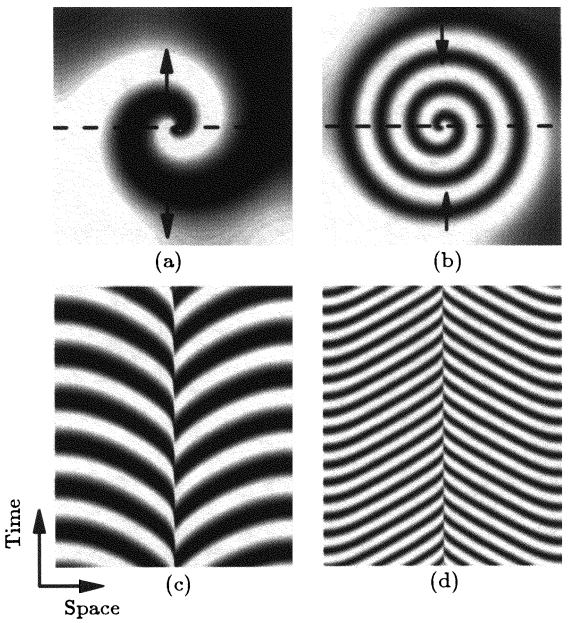


Fig.1. Snapshots (top) and time evolutions (bottom), propagating spirals [(a) and (c)] and anti-spiral waves [(b) and (d)]. The space–time representation of (c) and (d) corresponds, respectively, to the time evolution of the dashed cutlines marked in (a) and (b). Parameters: $a = 7.5$, $b = 0.8$, $D_{x'} = 0.07$ and $D_{y'} = 0.095$ for [(a) and (c)], $a = 16.0$, $b = 8.0$, $D_{x'} = 0.07$ and $D_{y'} = 0.075$ for [(b) and (d)]. The results are obtained by integrating Eq.(3) numerically under the zero-flux boundary condition on a 256×256 lattice by the two-step Lax–Wendroff algorithm, with grid space $h = 2.0$, time step $\Delta t = 0.02$.

If one changes the control parameters of the CIMA RD system away from the onset of Hopf bifurcation, pattern behaviour in the RD system can not be described by the CGLE any more. In order to observe where the CGLE fails to describe the corresponding RD system, we conducted a systematic study in numerical simulations of the dimensionless CIMA model, continuously changing the control parameter from near to far from the onset of the Hopf bifurcation. The results of these simulations is summarized in Fig.2. Figures 2(a) and 2(b) compare the behaviour of the CIMA RD system (a) and the corresponding CGLE (b). Values of $b_c - b$ measures the distance to the onset of Hopf bifurcation in the CIMA RD system; values of β is calculated from Eq.(10). Figure 2(b) shows that for CGLE prediction, anti-spirals should appear in the selected control parameters of the CIMA RD system. The direct simulations of CIMA RD system show that this is true only when the system being near the Hopf onset. From Fig.2(a), one observes that near the Hopf threshold, the observed behaviour in the CIMA RD system is indeed anti-spiral waves, consistent with the prediction of the CGLE in Fig.2(b). However, as the system moves far enough from Hopf onset, i.e., when $b_c - b$ is larger than 1.0, the prediction of the CGLE breaks down. In this case, spirals rather than anti-spirals take place in the CIMA reaction. This breaking down of prediction is clearly shown in Fig.2(c). In this figure, CIMA simulations are carried out by setting $b = 6.0$, and changing a from 13.5 to 15.5 for different pairs of diffusion coefficients: $D_{x'} = 0.070$, $D_{y'} = 0.075$; $D_{x'} = 0.070$, $D_{y'} = 0.070$; and $D_{x'} = 0.075$, $D_{y'} = 0.070$. The results are mapped to the (α, β) parameter plane to compare with the prediction of CGLE. The CGLE predicts that the white region in the figure should be a regime of anti-spirals, but for the corresponding CIMA RD system, a line of spiral–anti-spiral transition is obtained inside the white region, where the distance from the Hopf onset is large. Quantitative differences also exist between the CIMA RD system and the CGLE. For example, oscillation frequency simulated in the CIMA RD system increases with $b_c - b$, while it is a decreasing function of $b_c - b$ predicted by Eq.(14). This difference is shown in Fig.2(d). When $b_c - b$ is larger than 1.0 and the travelling waves change from anti-spirals to spirals, there is a striking dissimilarity between simulations and calculation from Eq.(14).

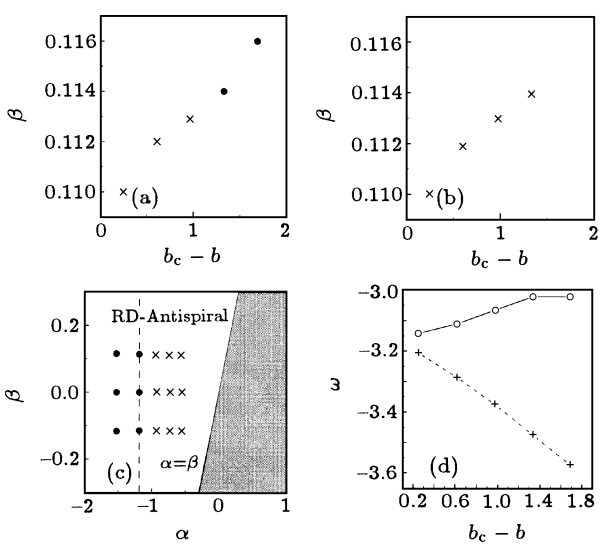


Fig.2. The relation between the CIMA reaction and the CGLE system for $b = 6.0$. (a) Parameter space $(\beta, b_c - b)$ for the CIMA reaction when changing a from 13.5 to 15.5; $D_{x'} = 0.070$, $D_{y'} = 0.075$. (b) Parameter space $(\beta, b_c - b)$ for the corresponding CGLE. (c) Comparison of spiral–anti-spiral transition between CIMA simulations and the CGLE prediction. (d) Frequency relationship between simulation results of the CIMA reaction (○)and calculation from the theory (+). Symbols: (•) for spiral, (×) for anti-spiral.

4. Discussion and conclusion

The major cause of the difference between the CGLE and the corresponding RD system is that we assume the Eq.(11) can represent the oscillations of the RD system. This assumption omits influence of higher harmonics of the oscillatory system, thus it is valid only when the RD system is near the supercritical Hopf bifurcation. As the system moves beyond the Hopf onset, higher harmonics become important. We suggest that this is the main cause of the spiral–anti-spiral transition and the CGLE breaking down. Figure 3 compares the oscillation modes of the RD system when it is near and far away from the onset of Hopf bifurcation. Near the Hopf instability, the oscillations in CIMA reaction is sinusoidal, as shown in Fig.3(a), which is quite different from the highly inharmonic oscillations observed when the system is apart from the onset, as shown in Fig.3(c). Figures 3(b) and 3(d) are the corresponding limit cycle motion that the CIMA system follows. Obviously, CGLE can only be applied to describe the sinusoidal oscillation when CIMA reaction is near the Hopf instability. Apart from the onset, the CGLE is no longer valid because the CIMA reaction makes the relaxation oscillation.

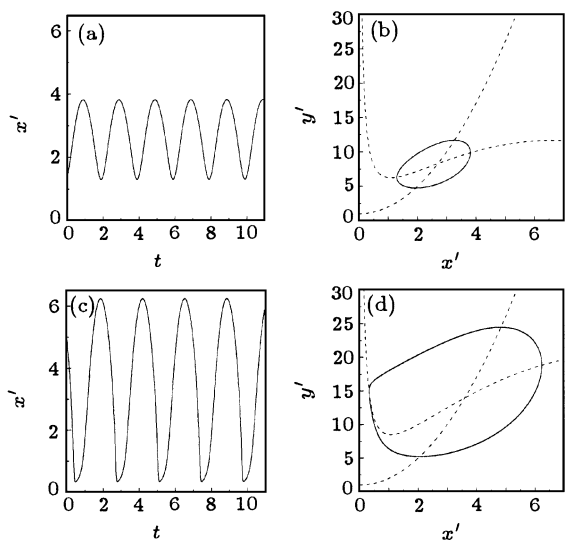


Fig.3. CIMA numerical simulations for $b = 6.0$, $D_{x'} = 0.070$, and $D_{y'} = 0.075$. (a) Time history of the variable x' when $a = 13.5$, where the CIMA reaction makes sinusoidal oscillation; and (b) shows the corresponding limit cycle(the solid line) the CIMA follows. (c) Time history of the variable x' when $a = 18.0$, where the CIMA reaction makes relaxation oscillation; and (d) shows the corresponding limit cycle(the solid line) the CIMA reaction follows.

In summary, to throw some light on the validity of the complex Ginzburg–Landau approximation, we have compared a RD system with their CGLE approximations. For the chemical RD system based on the CIMA reaction, we found that there exists substantial regions where the CGLE provides an excellent description of the dynamical behaviour. Spirals and anti-spirals in real chemical systems can be described by a CGLE with parameters α and β determined by the classic reductive perturbation method. However, the CGLE only applies to a coefficient region where the system is close to the Hopf bifurcation. We demonstrated how the CGLE approximation eventually fails beyond a certain limit. In this case, anti-spirals can not be found any more because the system follows the relaxation oscillation. In conclusion, the CGLE is just an approximation to the real chemical RD system close to the Hopf onset. The approximation is no longer valid when the chemical system is apart from the onset.

Acknowledgement

We thank Cheng X, Wang C and Wang S for helpful discussion.

References

[1] Aranson I S and Kramer L 2002 *Rev. Mod. Phys.* **74** 99
[2] Cross M C and Hohenberg P C 1993 *Rev. Mod. Phys.* **65** 851
[3] Kuramoto Y 1984 *Chemical Oscillations, Waves, and Turbulence* (Berlin: Springer)
[4] Nicolis G 1993 *Introduction to Nonlinear Science* (Cambridge: Cambridge University Press)
[5] Gong Y and Christini D J 2003 *Phys. Rev. Lett.* **90** 088302
[6] Vanag V K and Epstein I R 2001 *Science* **294** 835
[7] Vanag V K and Epstein I R 2002 *Phys. Rev. Lett.* **88** 088303
[8] Wang H L and Ouyang Q 2004 *Chin. Phys. Lett.* **21** 1437
[9] Nicola E M, Brush L and Bär M 2004 *Phys. Rev. Lett.* **92** 089801
[10] Nicola E M, Brush L and Bär M 2004 *J. Phys. Chem.* B **108** 14733
[11] Ipsen M, Hynne F and Sørensen P G 1997 *J. Bifur. Chaos* **7** 1539
[12] Lengyel I, Rabai G and Epstein I R 1990 *J. Am. Chem. Soc.* **90** 7863
[13] Lengyel I and Epstein I R 1991 *Science* **251** 650
[14] Lengyel I, Kadar S and Epstein I R 1992 *Phys. Rev. Lett.* **69** 2729
[15] Hagan P S 1982 *SIAM J. Appl. Math.* **42** 762